

HUMAN VS OBJECTIVE EVALUATION OF COLOURISATION PERFORMANCE

Seán Mullery
Institute of Technology, Sligo
Sligo
mullery.sean@itsligo.ie

Paul F. Whelan
Vision Systems Group
Dublin City University
Dublin
paul.whelan@dcu.ie

ABSTRACT

Automatic colourisation of grey-scale images is the process of creating a full-colour image from the grey-scale prior. It is an ill-posed problem, as there are many plausible colourisations for a given grey-scale prior. The current SOTA in auto-colourisation involves image-to-image type Deep Convolutional Neural Networks with Generative Adversarial Networks showing the greatest promise. The end goal of colourisation is to produce full colour images that appear plausible to the human viewer, but human assessment is costly and time consuming. This work assesses how well commonly used objective measures correlate with human opinion. We also attempt to determine what facets of colourisation have the most significant effect on human opinion. For each of 20 images from the BSD dataset, we create 65 recolourisations made up of local and global changes. Opinion scores are then crowd sourced using the Amazon Mechanical Turk and together with the images this forms an extensible dataset called the Human Evaluated Colourisation Dataset (HECD). While we find statistically significant correlations between human-opinion scores and a small number of objective measures, the strength of the correlations is low. There is also evidence that human observers are most intolerant to an incorrect hue of naturally occurring objects.

1 Introduction

The goal of automatic colourisation is to convert grey-scale images to colour images. Colourisation is an ill-posed problem as many plausible colourisations can result from the same grey-scale image. Predicting the exact colour of the original scene is impossible without further prior information from historical sources. A recent trend is to take any natural colour image dataset, convert it to a luminance-chrominance colour space, use the luminance channel as the grey-scale image and use the two chrominance channels as the ground-truth that a deep neural network must predict. This admits only a single ground-truth for each grey-scale image despite other plausible colourisations existing. Objective assessment of a colourisation model's predictions generally relies on distance measures from the ground-truth image.

In this paper we wish to answer the following questions.

- Do commonly used objective measures of colourisation performance correlate with mean human opinion scores?
- Is the ground-truth the perfect colourisation for its grey-scale prior?
- Will correction of white-balance of ground-truth images lead to higher opinion score?
- Are there any image statistics that all plausible colourisations might have in common?

Our key contributions are:

- An extensible Human Evaluated Colourisation dataset of recolourisations with matching human-opinion scores to benchmark future objective measures of colourisation.

- An assessment of the correlation between the human-opinion score of colourisation performance and the objective measures used in the colourisation literature.
- Analysis and insight into aspects of colourisation that affect the human-opinion score.
- An interactive tool to allow other researchers to analyse the HECD dataset and its results - <https://github.com/seanmullery/HECD>

2 How is colourisation performance measured in the literature?

Most colourisation techniques rely on some form of human-visual inspection to determine efficacy, or for comparison to other techniques. Human-visual inspection can include qualitative analysis [Irony et al., 2005, Isola et al., 2017, Welsh et al., 2002, Yatziv and Sapiro, 2006, Zhang et al., 2016, Zhang et al., 2017, An et al., 2019, Su et al., 2020, Li et al., 2019, Amelie Royer and Lampert, 2017, Górriz et al., 2019, Lee et al., 2020, Cao et al., 2017, Yoo et al., 2019], naturalness scoring [An et al., 2019, Iizuka et al., 2016, Zhao et al., 2018], user preference between two options [Li et al., 2019], Visual Turing Test (VTT) judged by human [Zhang et al., 2016, Zhang et al., 2017, Cao et al., 2017, Guadarrama et al., 2017], which of two colourisations best match a reference image’s colour [Li et al., 2019], or which, from many images, appears closest to a ground-truth [Yoo et al., 2019].

Many attempt an objective measure based on absolute pixel value errors, such as RMSE (Root Mean Squared Error) or L_2 pixel distance [Zhang et al., 2016, An et al., 2019, Deshpande et al., 2015, Deshpande et al., 2017], MAE (Mean Absolute Error) or L_1 pixel distance [Górriz et al., 2019], and PSNR (Peak Signal to Noise Ratio) [Zhang et al., 2017, Su et al., 2020, Górriz et al., 2019, Zhao et al., 2018, Cheng et al., 2015, Kim et al., 2021, Özbek, 2019]. [Lee et al., 2020] develop a patch based version of PSNR called SC-PSNR (Semantically Corresponding PSNR), as they wish to compare colour to a semantically similar patch from a reference image. SSIM (Structural Similarity Index Measure) [Wang et al., 2004], is used by [Su et al., 2020, Özbek, 2019, Zhao et al., 2020] and its multi-scale version MS-SSIM [Wang et al., 2003] is used by [Wu et al., 2019].

[Kim et al., 2021] developed an objective measure called CDR (Cluster Discrepancy Ratio) based on SLIC (Simple Linear Iterative Clustering) superpixels [Achanta et al., 2012]. CDR is formulated by looking at the discrepancy between super-pixel assignment for ground-truth versus colourisation. Similarly, [Zhao et al., 2018] use mean IoU of segmentation results on the PASCAL VOC2012 dataset [Everingham et al., 2012].

[Wu et al., 2021] use a no-reference measure called colourfulness score [Hasler and Süssstrunk, 2003] which incorporates the means and standard deviations of the a^* and b^* channels of CIEL*a*b* in a parametric model to compute a measure of how colourful the image is. The parameters were learned from data based on psychophysical experiments .

[Górriz et al., 2019] and [Guadarrama et al., 2017] compare histograms in the a^* and b^* channels of CIEL*a*b* over a distribution of images.

Some methods, [Zhang et al., 2016, Larsson et al., 2016, Vitoria et al., 2020], utilise the concept that colour will assist in classifying objects. Therefore a neural network designed to classify objects using colour images will show a deterioration in performance if inferred with a poorly colourised image. The difference can then be used as a proxy measure for colourisation performance. [Górriz et al., 2019] compare L_1 distance between convolutional features in the VGG19 model [Simonyan and Zisserman, 2015] for ground-truth and colourised samples. Similarly, [Lee et al., 2020] and [Wu et al., 2021] use Fréchet Inception Distance [Heusel et al., 2017], which requires comparing the inception score for colourisations versus ground-truth for 50K samples. [Zhang et al., 2018], developed a perception measure based on the features of deep neural networks called the Learned Perceptual Image Patch Similarity (LPIPS) metric, and this has also been used for the measure of colourisation in [Su et al., 2020, Yoo et al., 2019, Kim et al., 2021].

The work of [Anwar et al., 2020] is the only work we have found which attempt a dataset that is specifically designed for colourisation. Their dataset is designed with the idea of restricting synthetic objects or natural objects such as flowers that may have a wide distribution of plausible colours. Instead they include only natural objects that would be considered to have a narrow distribution of plausible colours such as specific types of fruit and vegetables. The images contain only a single object type, against a white background. There are 20 categories and 723 images in all. They then use PSNR, SSIM, PCQI (Patch-based contrast quality index), and UIQM (Underwater Image Quality Metric) to test out SOTA algorithms on their dataset. As is explained in section 3, our dataset design is considerably different and includes human evaluation data for each image.

3 The Human Evaluated Colourisation Dataset

The Human Evaluated Colourisation Dataset is based on 20 images from the Berkeley Segmentation Dataset [Martin et al., 2001]. From each of these 20, 65 images are created that differ in colour from the original. While we attempt to make changes that will be interpretable later, our primary objective is to have many different colour versions for human evaluation to allow appropriate comparison to objective measures. In total, $65 \times 20 = 1300$ and 20 original images will

result in a total of 1320 images in the set. The BSD set was chosen, as it has a variety of natural images and multiple human segmentations of each. The segmentations, in many cases, segment colour sections, allowing the alteration of the colour of specific sections without modification of the rest of the image. The original image will be referred to as the ground-truth from here on. The following changes are made to the ground-truth to create the HECD dataset. The first recolour modification is to auto-white-balance correct the 20 ground-truth images in Photoshop [Adobe, 2021], creating 20 new images. To ensure that Photoshop has not changed the L*-channel, the L*-channel is replaced with the ground-truth to ensure that only changes are made to a*b*. While the a*b* channels are close to perceptually uniform, they are not very intuitive, so a reformulation of these channels to hue and chroma channels is used via the equations of [Fairchild, 2013].

$$c = \sqrt{(a^*{}^2 + b^*{}^2)} \quad (1)$$

$$h = \tan^{-1}(b^*/a^*) \quad (2)$$

Where h is hue, and c is chroma. We now proceed to make the following global changes to the 40 images (20 ground-truth + 20 WB corrected). The changes below are arbitrary as there is no prior work to guide sample spacing or types of parameters:

- Alter intensity value of chroma by $\pm 2\sigma, \pm 1\sigma$ of the chroma of the image ($4 \times 40 = 160$ images).
- Alter contrast of chroma by $\frac{1}{4}, \frac{1}{2}, 2, 4$ ($4 \times 40 = 160$ images).
- Shift (offset registration) the a*b* channels spatially relative to the L*-channel by 0.01, 0.02, 0.03, 0.04 of the width and height of the image ($4 \times 40 = 160$ images). The edges that had no donor pixels, just retain their original value.
- Collect some SOTA colourisation algorithms' predictions of colour given the L*-channels of the 20 ground-truth images. The choice of which SOTA methods to include was based on availability of implementation and ability to accept the BSD image sizes without modification. The six methods chosen were, Photoshop Neural Filter [Adobe, 2021], Deoldify [Antic, 2021], available on MyHeritage.com, [Larsson et al., 2016], [Zhang et al., 2016], [Zhang et al., 2017] (using straight-forward inference with no user guidance), and [Iizuka et al., 2016]. We also replace these L*-channels with the ground-truth L*-channel in case any of the SOTA algorithms alter the L*-channel as part of their processing pipeline. $6 \times 20 = 120$ images.

In addition to the global changes, we also introduce some local changes. For each of the 40 images, we choose either a single segment or multiple segments that are of the same colour and make the following modifications to just the chosen segment(s).

- For the segment we alter the intensity of the chroma by $\pm 2\sigma, \pm 1\sigma$ of the chroma of the image ($4 \times 40 = 160$ images).
- Hue is not a magnitude space; you cannot have an absence of hue or more/less hue, and all hues are equally important. Therefore, statistics like mean and standard deviation are not meaningful in the hue channel. We alter the hue of the segment in a logarithmic fashion so that we can get better resolution in results closely surrounding the reference hue but still cover the full space of hue values without the cost of sampling all 256 hue values. Future extensions could more tightly sample the whole space. With the hue from Equation 2 forming a circular space $\in [0, 255]$ we make the following alterations from the reference hue. $\pm 2, \pm 4, \pm 8, \pm 16, \pm 32, \pm 64$, and 128 (± 128 results in the same change). ($13 \times 40 = 520$ images).

While this is a small dataset by current standards, it has been designed with extensibility in mind. The arbitrary modifications above were chosen to return the most information for the available resources. More ground-truth images and more recolour modifications along with tighter sampling between modification types, could be added in the future by collecting data in a manner consistent with that given in section 4.

4 Collecting the data.

The Amazon Mechanical Turk was used to assess human opinion on colourisation. Ethics approval was obtained in accordance with the University's Research Ethics Committee guidelines. Each assessment consisted of three images appearing on the screen simultaneously: the L*-channel (in the middle) and a colourisation on each side. One of the colourisations is the ground-truth colour image, and the other is one of the modifications described in section 3, see Figure 1. In this manner, all scores have a control in common. The observer is not informed that one image is the ground-truth and the positions vary in a pseudo-random manner so that there is an equal likelihood that the ground-truth could be on the left or the right. The user is asked to score the two colour images on naturalness (how much the colour looks like it would appear in real life). The scores are from 1-5 on an ordinal scale. Each observer rates 20 pairs.

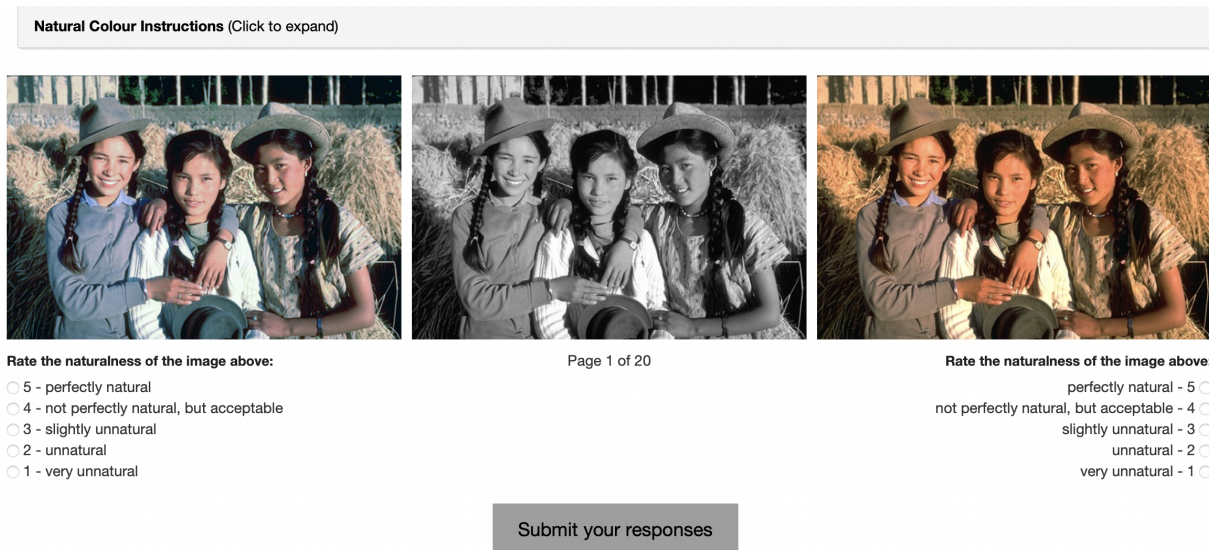


Figure 1: Each survey question displays three images. In the middle is the L^* -channel, which is common to the three images. On either side are the ground-truth and a recolourisation. The participants are not informed that one image is the ground-truth and it could appear on either right or left with equal probability. The participant must respond to both before continuing.

They see each of the 20 ground-truth images in the dataset and a recoloured version. For any set of 20, the type of recolourisation is pseudo-random, so the user does not become accustomed to the type of colour change. As there are 65 recolour versions, 65 surveys of 20 comparisons are created for 1300 responses in total. While each survey is pseudo-random internally, the actual survey is identical for each observer that responds to it. We do not allow a participant to respond to a unique survey twice. In general, we allow participants to complete only one survey. A small number completed two different surveys (19 participants). This is not a problem, but if participants were allowed to do many surveys in a short period, it could lead to non-naivete, with the participant learning that specific colour versions appear in all surveys, i.e. they may learn to recognise the ground-truth and be biased towards awarding it the higher of the two scores. In all, there were 1281 participants. Twenty participants completed each survey. Twenty-nine incomplete surveys were not used but also not counted in the total 1300 complete surveys. In surveys with more than one response for a pair of images (respondent used the back button in the browser), the final result was used on the assumption that this is what the respondent intended. There were 25 surveys where the user gave the same value for all answers (straight-lining) and 15 where the respondent gave the same number for the two images under consideration in all 20 comparisons; these were removed from the data, leaving 1260 complete surveys.

5 Processing the raw numbers

As the ground-truth image was used as the control, it is the difference between the score for the ground-truth and the recoloured image in which we are interested. However, account for differences in individual participants that may bias the results still needs to be taken. One participant may score all pairs lower than another participant, with all else equal. As the ordinal values for scoring and the gaps between them are subjective, two participants who perceive the same difference between two images may still give a larger/smaller difference in scores compared to each other. Differences in viewing equipment/environment may also have systematic effects between two respondents. For this reason, it is necessary to consider the trend for the participant as a whole over the 20 image pairs to which they respond. The method of [Sheikh et al., 2006] can then be used to calculate the difference for each pair.

$$d_{ij} = r_{ij} - r_{iref(j)} \quad (3)$$

where r_{ij} is the raw score for the i -th participant and j -th image, and $r_{iref(j)}$ denotes the raw quality score assigned by the i -th participant to the reference image corresponding to the j -th recolourised image. The raw difference scores d_{ij} for the i -th participant and j -th image are converted into Z-scores.

$$z_{ij} = (d_{ij} - \bar{d}_i) / \sigma_i \quad (4)$$

Table 1: Spearman rank order correlation for all reference images individually and all combined. The numbers represent the Spearman-r value, and the shaded numbers are those that are statistically significant with a p-value < 0.05. The best performer in each row is shown in bold.

GT File Name	SSIM (a*b*)	SSIM (hc)	SSIM (rgb)	MS-SSIM (a*b*)	MS-SSIM (hc)	MS-SSIM (rgb)	MSE (a*b*)	MSE (hc)	RMSE (a*b*)	RMSE (hc)	MAE (a*b*)	MAE (hc)	Colourfulness	Colourfulness-dif	psnr-ab	psnr-hc	CDR	lpiips-vgg	lpiips-alex
015004_gt.jpg	0.298	0.165	0.165	0.444	0.242	0.399	-0.294	0.118	-0.292	0.123	0.198	-0.029	-0.228	-0.228	0.367	0.115	-0.261	-0.291	-0.352
022090_gt.jpg	0.303	0.022	0.022	0.29	0.091	0.331	-0.121	0.06	-0.136	0.062	-0.183	-0.082	-0.078	-0.078	0.096	-0.078	-0.178	-0.114	-0.125
022093_gt.jpg	0.364	0.189	0.189	0.468	0.179	0.377	-0.225	-0.296	-0.211	-0.271	-0.437	-0.124	0.411	0.411	0.374	-0.075	-0.295	-0.165	-0.267
024004_gt.jpg	0.498	0.504	0.504	0.598	0.536	0.541	-0.401	-0.23	-0.434	-0.022	-0.459	-0.145	0.098	0.098	0.512	0.259	-0.457	-0.538	-0.502
025098_gt.jpg	0.37	0.193	0.193	0.457	0.099	0.487	-0.363	-0.088	-0.41	-0.032	0.055	0.457	0.018	0.018	0.568	0.069	-0.34	-0.369	-0.395
046076_gt.jpg	0.418	0.062	0.062	0.547	0.042	0.441	-0.194	-0.331	-0.209	-0.262	0.126	0.16	0.125	0.125	0.402	-0.101	-0.27	-0.314	-0.454
056028_gt.jpg	0.283	0.193	0.193	0.34	0.139	0.302	-0.219	-0.021	-0.255	0.093	-0.21	0.179	-0.195	-0.195	0.23	0.035	-0.243	-0.384	-0.368
065019_gt.jpg	0.443	0.6	0.6	0.386	0.636	0.444	-0.426	-0.282	-0.43	-0.285	-0.308	-0.428	0.215	0.215	0.346	0.538	-0.533	-0.399	-0.337
078019_gt.jpg	0.577	0.628	0.628	0.64	0.66	0.585	-0.617	0.212	-0.61	0.34	-0.112	0.504	-0.238	-0.238	0.561	0.685	-0.539	-0.602	-0.589
118020_gt.jpg	0.511	0.33	0.33	0.594	0.281	0.582	-0.517	-0.018	-0.508	0.023	-0.075	0.143	-0.321	-0.321	0.526	0.043	-0.448	-0.539	-0.513
118035_gt.jpg	0.673	0.489	0.489	0.694	0.626	0.617	-0.612	-0.315	-0.607	-0.254	0.177	0.445	-0.472	-0.472	0.565	0.651	-0.51	-0.596	-0.569
140075_gt.jpg	0.627	0.436	0.436	0.651	0.386	0.627	-0.6	-0.325	-0.611	-0.252	-0.176	-0.089	0.157	0.157	0.405	0.29	-0.438	-0.586	-0.545
151087_gt.jpg	0.633	0.57	0.57	0.65	0.597	0.618	-0.608	0.183	-0.608	0.19	0.0	0.061	-0.023	-0.023	0.611	0.299	-0.579	-0.583	-0.559
153093_gt.jpg	0.561	0.458	0.458	0.647	0.206	0.621	-0.28	0.029	-0.354	0.201	0.043	0.275	-0.112	-0.112	0.394	0.106	-0.728	-0.717	-0.709
187029_gt.jpg	0.545	0.338	0.338	0.522	0.39	0.541	-0.314	0.153	-0.354	0.172	0.025	0.48	0.273	0.273	0.538	0.053	-0.513	-0.527	-0.529
198023_gt.jpg	0.539	0.327	0.327	0.648	-0.034	0.667	-0.58	0.429	-0.589	0.433	0.218	0.468	-0.256	-0.256	0.608	-0.169	-0.694	-0.658	-0.726
239096_gt.jpg	0.578	0.585	0.585	0.532	0.438	0.583	-0.501	-0.258	-0.509	-0.138	-0.231	-0.002	0.012	0.012	0.455	0.192	-0.489	-0.604	-0.566
242078_gt.jpg	0.509	0.424	0.424	0.531	0.351	0.584	-0.441	-0.299	-0.422	-0.192	-0.072	0.032	-0.057	-0.057	0.135	0.161	-0.524	-0.736	-0.725
323016_gt.jpg	0.642	0.247	0.247	0.724	0.332	0.7	-0.531	0.172	-0.515	0.118	0.082	-0.315	-0.314	-0.314	0.496	0.315	-0.481	-0.57	-0.653
376001_gt.jpg	0.318	0.279	0.279	0.315	0.234	0.448	-0.238	-0.063	-0.245	-0.068	0.085	-0.057	-0.039	-0.039	0.378	0.129	-0.399	-0.394	-0.424
All	0.492	0.271	0.422	0.567	0.29	0.549	-0.416	0.015	-0.434	0.091	-0.135	0.034	-0.022	0.071	0.45	0.068	-0.461	-0.474	-0.495

Where \bar{d}_i is the mean of the raw difference scores over all of the images ranked by participant i , and σ_i is the standard deviation of the differences for participant i . z_{ij} then represents a score for an image j by participant i . In most cases, in this document, the score for an image j is given as the mean over all the participants that responded to it. Because the ground-truth is used as the control and the processing is based on the statistics of the participants, the ground-truth images are all considered of equal quality. When their z-scores are calculated and averaged, they all come to the same value. As there were more recolourisations that scored lower than the ground-truth than those scoring higher, the average score for the ground-truth will have a positive non-zero value.

6 Results

6.1 How do objective measures correlate with human opinion?

As outlined in section 2, colourisation researchers have attempted to use many different types of objective measures to assess the quality of colourisations. We test if the human scores correlate with the commonly used objective measures. As ordinal data is used, two rank-order correlation measures will be used to examine the rank order correlation of the results, namely Spearman-r [Spearman, 1904], see table 1 and Kendall-tau [Kendall, 1938], see table 2. The shaded values, in the tables, represent values where the p-value of the rank-order correlation was less than 0.05, indicating statistical significance. We test against SSIM [Wang et al., 2004], MS-SSIM [Wang et al., 2003], MSE, RMSE/ L_2 , MAE/ L_1 , Colourfulness and Colourfulness Difference [Hasler and Süssstrunk, 2003], PSNR, CDR [Kim et al., 2021] and LPIPS [Zhang et al., 2018] for both VGG [Simonyan and Zisserman, 2015] and Alexnet [Krizhevsky et al., 2012]. We cannot test FID [Heusel et al., 2017], or SC-PSNR [Lee et al., 2020], as they require different data than we have used for the surveys. Where possible, we use established libraries for the measures. SKImage [Van der Walt et al., 2014] for SSIM and PSNR, Searw [Khalel and contributors, 2020] for MS-SSIM, RMSE (L_2), and MSE, and SKLearn [Pedregosa et al., 2011] for MAE (L_1). Colourfulness and Colourfulness-Difference are developed from the details in [Hasler and Süssstrunk, 2003]. CDR is developed from the details in [Kim et al., 2021] and relies on SKImage’s SLIC library. We also test in three different colour spaces where the method is not specific to a particular colour space, namely a*b*, hc (see Equations 1 and 2) and RGB. a*b* and hc do not include the L*-channel in the comparison as L* is common in all pairings. RGB incorporates the L*-channel but in a different formulation. We can see from tables 1 and 2 that MS-SSIM, when used with either a*b* or RGB, has the strongest correlation with human judgement. Standard SSIM with a*b* is the only other that has a statistically significant correlation for all images. hc seems to be a poor space in which to use any of the objective measures despite most of the changes in our dataset being made in this formulation, see section 3. Even for the top performer, MS-SSIM with a*b*, the correlation for the complete set with Spearman is 0.567 and Kendall is 0.389. In general, values above 0.7 are considered “Strong Correlation”, so none of the objective measures meets that threshold, though a small number do reach this for an individual image. In short, the objective measures employed in the literature do not work well for colourisation. There is scope here for a more targeted objective measure, and our HECD dataset is publicly available to help in this search.

Table 2: Kendall rank order correlation for all reference images individually and all combined. The numbers represent the Kendall tau value, and the shaded numbers are those that are statistically significant with a p-value < 0.05. The best performer in each row is shown in bold.

GT File Name	SSIM (a*b*)	SSIM (hc)	SSIM (rgb)	MS-SSIM (a*b*)	MS-SSIM (hc)	MS-SSIM (rgb)	MSE (a*b*)	MSE (hc)	RMSE (a*b*)	RMSE (hc)	MAE (a*b*)	MAE (hc)	Colourfulness	Colourfulness-dif	psnr-ab	psnr-hc	CDR	lipps-veg	lipps-alex
015004_gt.jpg	0.205	0.098	0.098	0.299	0.158	0.28	-0.194	0.075	-0.191	0.083	0.126	-0.014	-0.161	0.161	0.247	0.076	-0.19	-0.201	-0.234
022090_gt.jpg	0.205	0.016	0.016	0.197	0.071	0.215	-0.093	0.051	-0.104	0.055	-0.123	-0.072	-0.055	0.055	0.075	-0.058	-0.122	-0.083	-0.085
022093_gt.jpg	0.245	0.128	0.128	0.31	0.125	0.248	-0.149	-0.201	-0.145	-0.187	-0.306	-0.087	0.294	-0.294	0.241	-0.032	-0.217	-0.114	-0.192
024004_gt.jpg	0.35	0.351	0.351	0.425	0.371	0.38	-0.273	-0.169	-0.3	-0.025	-0.314	-0.085	0.07	-0.07	0.344	0.186	-0.316	-0.376	-0.346
025098_gt.jpg	0.27	0.138	0.138	0.333	0.072	0.342	-0.251	-0.065	-0.283	-0.032	0.031	0.316	0.012	-0.012	0.398	0.049	-0.243	-0.254	-0.271
046076_gt.jpg	0.276	0.063	0.063	0.378	0.044	0.295	-0.128	-0.235	-0.141	-0.191	0.096	0.123	0.101	-0.101	0.273	-0.02	-0.179	-0.21	-0.303
056028_gt.jpg	0.18	0.133	0.133	0.216	0.101	0.198	-0.152	-0.013	-0.174	0.065	-0.153	0.131	-0.138	0.138	0.142	0.027	-0.159	-0.265	-0.253
065019_gt.jpg	0.319	0.423	0.423	0.276	0.458	0.327	-0.29	-0.198	-0.293	-0.189	-0.193	-0.269	0.152	-0.152	0.241	0.373	-0.389	-0.302	-0.262
078019_gt.jpg	0.409	0.456	0.456	0.461	0.483	0.414	-0.43	0.141	-0.427	0.227	-0.097	0.357	-0.179	0.179	0.386	0.509	-0.38	-0.437	-0.432
118020_gt.jpg	0.35	0.229	0.229	0.412	0.215	0.401	-0.345	-0.028	-0.345	0	-0.055	0.1	-0.23	0.23	0.356	0.055	-0.309	-0.387	-0.359
118035_gt.jpg	0.476	0.325	0.325	0.485	0.433	0.447	-0.416	-0.227	-0.41	-0.175	0.119	0.303	-0.334	0.334	0.381	0.448	-0.362	-0.401	-0.404
140075_gt.jpg	0.448	0.305	0.305	0.473	0.267	0.441	-0.411	-0.231	-0.424	-0.183	-0.124	-0.066	0.098	-0.098	0.284	0.196	-0.302	-0.414	-0.37
151087_gt.jpg	0.437	0.37	0.37	0.451	0.404	0.42	-0.405	0.125	-0.404	0.134	0.002	0.051	-0.024	0.024	0.413	0.204	-0.397	-0.377	-0.356
153093_gt.jpg	0.401	0.316	0.316	0.468	0.118	0.45	-0.2	0.016	-0.262	0.136	0.023	0.175	-0.077	0.077	0.31	0.041	-0.545	-0.524	-0.514
187029_gt.jpg	0.371	0.228	0.228	0.352	0.263	0.371	-0.201	0.074	-0.226	0.076	0.011	0.361	0.221	-0.221	0.385	0.076	-0.357	-0.361	-0.367
198023_gt.jpg	0.372	0.242	0.242	0.458	0.001	0.48	-0.405	0.298	-0.415	0.303	0.131	0.319	-0.177	0.177	0.436	-0.106	-0.494	-0.459	-0.504
239096_gt.jpg	0.427	0.414	0.414	0.389	0.312	0.427	-0.383	-0.205	-0.39	-0.127	-0.132	-0.005	0.034	-0.034	0.344	0.127	-0.384	-0.463	-0.441
242078_gt.jpg	0.359	0.299	0.299	0.373	0.239	0.423	-0.313	-0.229	-0.292	-0.141	-0.043	0.014	-0.047	0.047	0.095	0.076	-0.367	-0.552	-0.527
323016_gt.jpg	0.446	0.153	0.153	0.521	0.212	0.492	-0.348	0.138	-0.334	0.107	0.056	-0.211	-0.221	0.221	0.317	0.216	-0.332	-0.375	-0.439
376001_gt.jpg	0.228	0.193	0.193	0.227	0.154	0.314	-0.167	-0.046	-0.174	-0.054	0.056	-0.03	-0.037	0.037	0.263	0.077	-0.279	-0.272	-0.298
All	0.334	0.181	0.283	0.389	0.194	0.375	-0.277	0.011	-0.289	0.063	-0.089	0.022	-0.015	-0.049	0.302	0.049	-0.315	-0.325	-0.341

6.2 Is the ground-truth the perfect colourisation for its grey-scale prior?

The method currently employed in most deep-learning colourisation systems is to take any natural image dataset, convert the images to CIEL*a*b*, then use the L*-channel as the prior (input) and predict the a*b* colour channels, with the colour channels from the dataset as the ground-truth. Figure 2 shows that human observers do not rate the ground-truth as higher than all other colour versions that were created in the dataset. Approximately 36% of the area is above the mean ground-truth score (to the right of the blue-dashed line). This shows that many more plausible colourisations of a scene exist than the ground-truth, but will, in current training regimes, be penalised for being different from the ground-truth.

The 20 ground-truth images in our dataset are quite good as they come from the BSD dataset. The images are not necessarily natural or high-quality in many commonly used large image datasets; They may be in black and white, duo-tone, or stylised. In classification models, these unnatural or poor quality images are a feature rather than a bug as the desire is to train models to recognise objects even in poor quality images. It therefore makes sense for poor quality images to have the same label as high-quality images if they contain the same object. For generative tasks, such as colourisation, when the task requires a model to generate high-quality colourisations, then poor colourisations in the dataset should not have an equal label to good ones. However, the lack of a reliable no-reference measure for the quality of a colourisation leaves little choice but to treat all images in a dataset as equal-maximum colourisation quality. The only alternative is to assess and sort the large training datasets by resource-intensive human visual inspection.

6.3 Does white-balance correction of the ground-truth image lead to higher opinion score?

Photoshop’s [Adobe, 2021] white-balance auto-correction was used to produce a white-balance corrected version of each ground-truth image. Using only the direct comparisons between the ground-truth images and WB corrected images resulted in a score of 0.376 for the white-balanced images and a mean of 0.364 for the ground-truth images. This difference is minimal and has a statistical significance of $p=0.058$, using the Mann-Whitney u-test [Mann and Whitney, 1947]. While the traditional threshold of $p < 0.05$ is arbitrary, the mean difference has not reached that threshold, and with such a slight difference in the value of the mean, white-balance correcting the images in a dataset before training will have only a minimal effect unless there is reason to believe the images in the dataset have particularly bad colour casts.

6.4 How do SOTA colourisation algorithms fair?

Six state-of-the-art colourisation algorithm’s outputs were included in the HECD dataset. The choice of algorithms was made primarily on the availability of implementation and the ability to accept the exact image dimensions used in BSD images. The results in Figure 3 and table 3 show that the two commercial products, DeOldify (from MyHeritage.com [Antic, 2021]) and Photoshop [Adobe, 2021], edge ahead of all the others, which are considerably less recent than the commercial products. DeOldify came top in the surveys, and the difference to Photoshop was

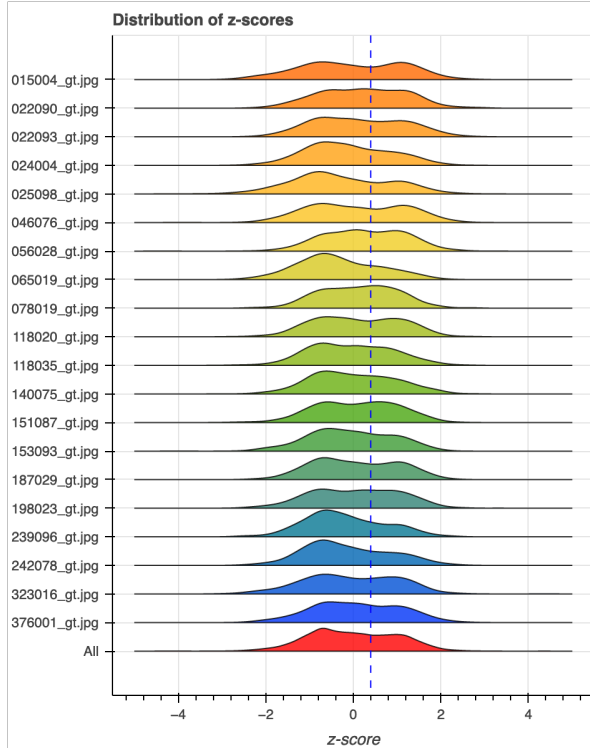


Figure 2: The distribution of responses after the processing in section 5 for all reference images individually and all together. The blue-dashed line shows the value for the ground-truth images. All ground-truth images are assumed equal as we grade on difference scores from the ground-truth. Any area under the curve to the right of the blue line represents scores where the participant gave the recoloured version a higher score than they gave the ground-truth. We can see that all references have a large area to the right of the ground-truth score. This shows that the ground-truth is far from the most plausible colourisation, as judged by human evaluation.

Table 3: Mean value Z-Score for the six SOTA methods that we tested, shown in descending order. The mean of the ground-truth when compared with the SOTA algorithms was 0.397.

SOTA Colourisation	Mean z-score
Ground-Truth	0.397
DeOldify	0.258
PhotoShop	0.001
Iizuka	-0.151
Larsson	-0.196
Zhang 2	-0.201
Zhang 1	-0.264

statistically significant with a p-value of 0.001, using the Mann-Whitney u-test [Mann and Whitney, 1947]. The mean score for the ground-truth images was still higher than the mean for any of the SOTA methods, table 3.

Many of the human-evaluation methods outlined in section 2 found that their method could fool a human evaluator or obtain a higher score from a human evaluator on some occasions. We also find this to be the case, as evidenced by the area under the curves in Figure 3 to the right of the dashed line. This area represents the proportion of samples from each model that achieved a higher score than the ground-truth when it and the ground-truth appeared together for comparison scoring.

6.5 Image Modification Statistics

Figure 4 shows the effect of making a single modification type to a reference image. These are all relative changes that should be understood in terms of the reference image. The L^* -channel is held fixed for all these modifications. Units, such as standard deviation, refer to the statistics of the reference image and so will represent a different absolute

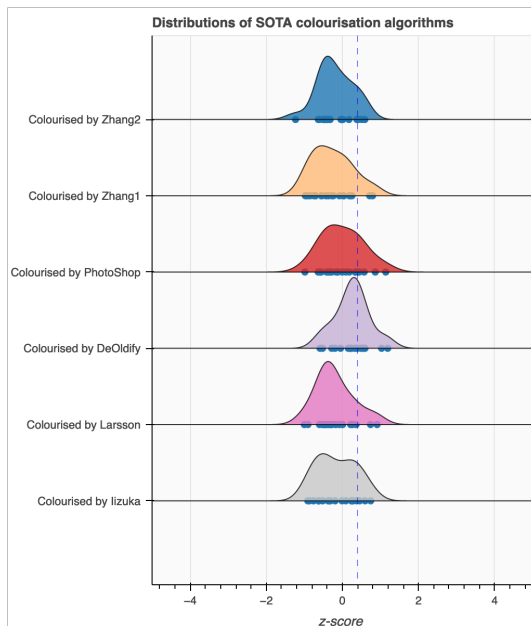


Figure 3: The blue dashed line shows the average Ground-Truth score, when compared against SOTA colourisations, of 0.397. This is higher than the average of the SOTA Colourisation methods, but we can see that all methods achieve some part of the distribution of their scores which is higher than the average ground-truth score. The blue dots represent the mean score of individual images. These can be explored further with our interactive tool.

value in each case. Figures 4 (a) and 4 (b) show that when the statistics of the chroma of a reference image change, this will, in general, cause a deterioration in mean opinion score, with the caveat that the participants seemed to prefer slightly higher chroma than the reference. Figure 4 (c) is the equivalent change to 4 (a) but for only a colour segment of the image, with results are similar but less pronounced, as the rest of the pixels in the image retain the reference statistics. Figure 4 (d) shows the effect of spatially shifting the colour channels relative to the L^* -channel, causing deterioration with an increase in spatial misalignment. However, it should be noted that slight misalignment leads to a relatively small drop in opinion score, particularly when we consider that all pixels are misaligned. We can extrapolate that local colour bleeding across boundaries in colourisations by a small number of pixels will have a relatively small impact on opinion score. Indeed chroma subsampling, widely used in image and video encoding, utilises the Human Visual System’s lower acuity in chroma. 4 (e) shows the effect of changing the hue of a segment. When the data is split into its two reference image categories, namely original ground-truth and white-balance corrected image derived from the ground truth, the responses of these are broadly similar. However, when the data is separated into hue changes to colour segments representing natural objects and those representing synthetic objects, a clear difference between the two groups emerges. Examples of natural objects are skin tones and foliage. Examples of synthetic objects are painted surfaces and textiles. Figure 4 (e) shows that both categories see a deterioration in opinion score with medium to large changes in hue for a segment. However, this deterioration is relatively small for synthetic segments compared to the large change for natural objects. While synthetic objects can theoretically take on any hue, there is still a drop in opinion score with large changes in hue for a colour segment. This may be because the L^* -channel prior and the surrounding colours (which did not change from the reference) constrain the most plausible hues to a small band of hue values close to the ground-truth. For colour segments of natural objects, the response is quite different. Small changes in hue to a natural segment may increase the mean opinion score. This may be that the small correction looks more plausible, but it could also be the inherent noise in opinion scores, particularly due to the more dense sampling close to the reference hue. However, the trend is that medium to large changes in natural segment hue sees a large deterioration in the mean opinion score. By directly comparing Figure 4 (e) with Figures 4 (a) and 4 (d) we can see that changing the hue of a natural segment by $64/256$ of the full-scale has an equivalent effect on the opinion score of misaligning the colour channels with L^* of 0.03 of the dimensions of the image and it has a greater effect than globally changing all of the chroma values by two standard deviations of the chroma in the reference image. This tells us that not all pixels are created equal in colourisation performance.

Human vs Objective Evaluation of Colourisation Performance

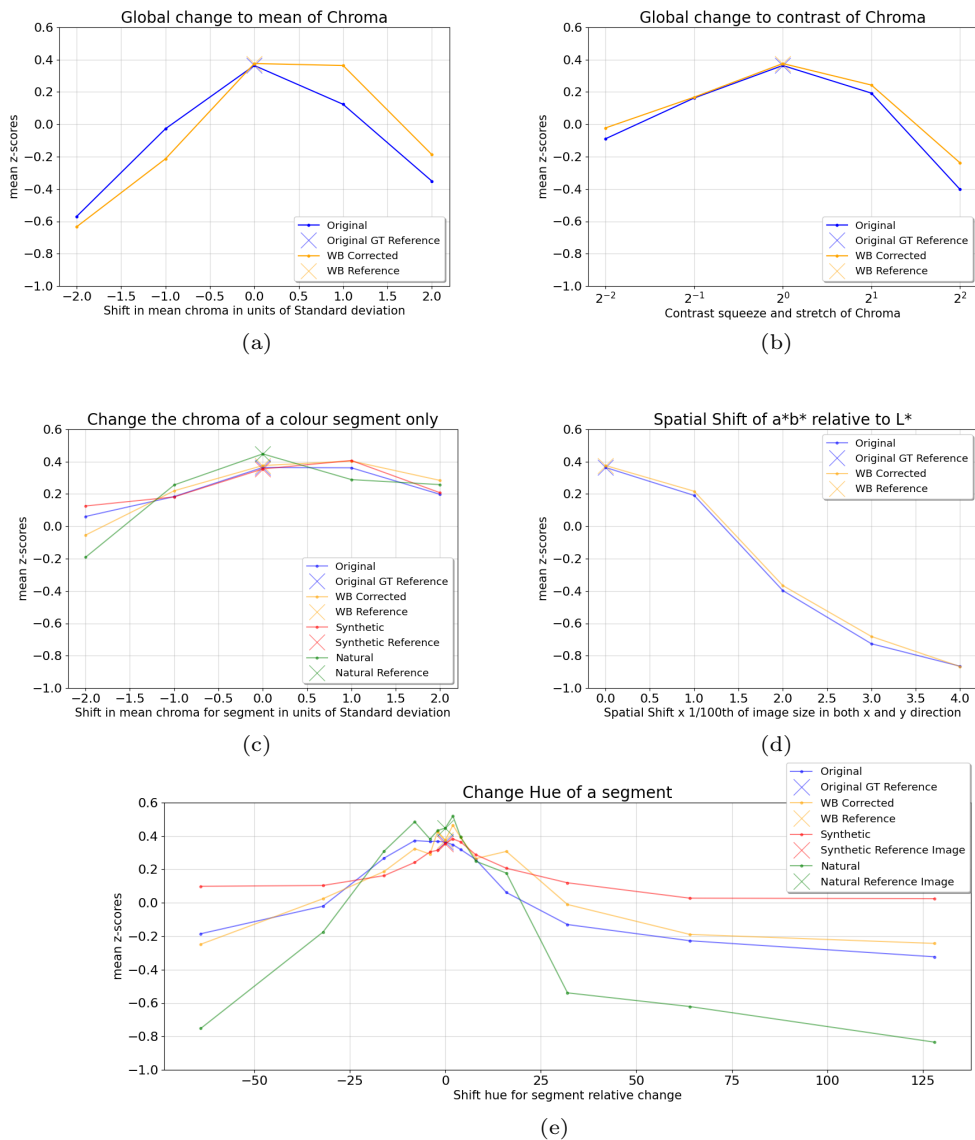


Figure 4: In the figure, are various subsets of the data relating to specific modifications, outlined in section 3, and the effect of those on mean opinion score. All graphs have the same y-scale (mean opinion z-score) so that comparisons of different types of change can be made at a glance. Sub-figures (a) and (b) look at relative global changes to the statistics of the chroma of the reference image. Sub-figure (c) is the equivalent of (a) but for changes to only a colour segment of an image, leaving all other pixels the same as the reference. (d) shows the effect of spatially shifting (misaligning) the colour channels relative to the L*-channel. (e) looks at the effect of changing the relative hue of a colour segment while leaving all other pixels unchanged from the reference. We look at two data slices for global changes, whether the recolour version derived from the original ground-truth or the white-balance corrected image. For segment modifications (c) and (e), we also look at those slices as well as slicing on whether the modified segment represented a natural or synthetic object.

7 Conclusion.

We have shown that the widely-used objective measures utilised in the colourisation literature do not correlate well with human opinion. MS-SSIM shows the highest correlation in our findings but is still too low to make it an appropriate gauge of colourisation quality.

The hue of natural objects stands out as significant to the human opinion of the naturalness of an image. Observers seem tolerant of minor differences in hue to natural objects, but medium to large changes are heavily penalised. The observers are relatively tolerant of all changes to the hue of synthetic objects.

There is a general trend towards a preference for more saturated (higher average chroma) images. Small increases to the chroma of the ground-truth images led to higher opinion scores, but increases beyond that led to a deterioration in opinion score, as did any decrease in the chroma from the ground-truth. The trends were similar when changes were only made to the chroma of small colour segments; The effects were smaller because only some pixels were affected by the change. However, the effect is not necessarily proportional to the number of pixels, as the observer may be guided by the discrepancy in chroma to the surrounding regions. Both increasing and decreasing the global contrast of chroma caused a deterioration in opinion scores.

The observers registered a slight change in opinion for small global registration discrepancies between the colour channels and the L^* -channel. Increasing deregistration led to a significant deterioration in opinion scores. This suggests some tolerance to small amounts of colour bleeding but intolerance to more significant amounts. We can assume some cross over with the hue of natural objects here; If de-registration problems change the hue of a natural object, we will again see a significant deterioration in opinion score.

Finally, caution should be exercised in simply treating all colour images in a data set as perfect colourisations. The results show that many versions in our limited set of arbitrary modifications scored higher than the ground-truth. Auto-white-balance correction of ground-truth images brought only a minor improvement on average, though it may bring a more significant improvement if the white-balance is poor in the ground-truth images.

References

- [Achanta et al., 2012] Achanta, R., Shaji, A., Smith, K., Lucchi, A., Fua, P., and Süsstrunk, S. (2012). Slic superpixels compared to state-of-the-art superpixel methods. *IEEE Transactions on Pattern Analysis and Machine Intelligence*, 34(11):2274–2282.
- [Adobe, 2021] Adobe (2021). Photoshop.
- [Amelie Royer and Lampert, 2017] Amelie Royer, A. K. and Lampert, C. (2017). Probabilistic image colorization. In Tae-Kyun Kim, Stefanos Zafeiriou, G. B. and Mikolajczyk, K., editors, *Proceedings of the British Machine Vision Conference (BMVC)*, pages 85.1–85.12, London. BMVA Press.
- [An et al., 2019] An, J., Gagnon, K. K., Shi, Q., Xie, H., and Cao, R. (2019). Image colorization with convolutional neural networks. In *2019 12th International Congress on Image and Signal Processing, BioMedical Engineering and Informatics (CISP-BMEI)*, pages 1–4, Suzhou. CISP-BMEI.
- [Antic, 2021] Antic, J. (2021). Colorize photos.
- [Anwar et al., 2020] Anwar, S., Tahir, M., Li, C., Mian, A. S., Khan, F. S., and Muzaffar, A. W. (2020). Image colorization: A survey and dataset. *ArXiv*, abs/2008.10774.
- [Cao et al., 2017] Cao, Y., Zhou, Z., Zhang, W., and Yu, Y. (2017). Unsupervised diverse colorization via generative adversarial networks.
- [Cheng et al., 2015] Cheng, Z., Yang, Q., and Sheng, B. (2015). Deep colorization. *2015 IEEE International Conference on Computer Vision (ICCV)*, 1(1):415–423.
- [Deshpande et al., 2017] Deshpande, A., Lu, J., Yeh, M., Chong, M. J., and Forsyth, D. (2017). Learning diverse image colorization. In *2017 IEEE Conference on Computer Vision and Pattern Recognition (CVPR)*, pages 2877–2885, Honolulu. IEEE.
- [Deshpande et al., 2015] Deshpande, A., Rock, J., and Forsyth, D. (2015). Learning large-scale automatic image colorization. In *2015 IEEE International Conference on Computer Vision (ICCV)*, pages 567–575, Santiago, Chile. IEEE.
- [Everingham et al., 2012] Everingham, M., Van Gool, L., Williams, C. K. I., Winn, J., and Zisserman, A. (2012). The PASCAL Visual Object Classes Challenge 2012 (VOC2012) Results. <http://www.pascal-network.org/challenges/VOC/voc2012/workshop/index.html>.
- [Fairchild, 2013] Fairchild, M. D. (2013). *Color Appearance Models*, chapter 10, pages 199–212. John Wiley & Sons, Ltd, Hoboken, New Jersey.

- [Guadarrama et al., 2017] Guadarrama, S., Dahl, R., Bieber, D., Shlens, J., Norouzi, M., and Murphy, K. (2017). Pixcolor: Pixel recursive colorization. In Tae-Kyun Kim, Stefanos Zafeiriou, G. B. and Mikolajczyk, K., editors, *Proceedings of the British Machine Vision Conference (BMVC)*, pages 112.1–112.13, London. BMVA Press.
- [Górriz et al., 2019] Górriz, M., Mrak, M., Smeaton, A. F., and O’Connor, N. E. (2019). End-to-end conditional gan-based architectures for image colourisation.
- [Hasler and Süsstrunk, 2003] Hasler, D. and Süsstrunk, S. (2003). Measuring colourfulness in natural images. *Proc. IS&T/SPIE Electronic Imaging 2003: Human Vision and Electronic Imaging VIII*, 5007:87–95.
- [Heusel et al., 2017] Heusel, M., Ramsauer, H., Unterthiner, T., Nessler, B., Klambauer, G., and Hochreiter, S. (2017). Gans trained by a two time-scale update rule converge to a nash equilibrium. *CoRR*, abs/1706.08500.
- [Iizuka et al., 2016] Iizuka, S., Simo-Serra, E., and Ishikawa, H. (2016). Let there be color!: Joint end-to-end learning of global and local image priors for automatic image colorization with simultaneous classification. *ACM Trans. Graph.*, 35(4):110:1–110:11.
- [Irony et al., 2005] Irony, R., Cohen-Or, D., and Lischinski, D. (2005). Colorization by example. In *Proceedings of the Sixteenth Eurographics Conference on Rendering Techniques, EGSR ’05*, pages 201–210, Aire-la-Ville, Switzerland, Switzerland. Eurographics Association.
- [Isola et al., 2017] Isola, P., Zhu, J. Y., Zhou, T., and Efros, A. A. (2017). Image-to-image translation with conditional adversarial networks. *Proceedings - 30th IEEE Conference on Computer Vision and Pattern Recognition, CVPR 2017*, 2017-January:5967–5976.
- [Kendall, 1938] Kendall, M. (1938). A new measure of rank correlation. *Biometrika*, 1(1).
- [Khalel and contributors, 2020] Khalel, A. and contributors (2020). Sewar: python package for image quality assessment using different metrics.
- [Kim et al., 2021] Kim, E., Lee, S., Park, J., Choi, S., Seo, C., and Choo, J. (2021). Deep edge-aware interactive colorization against color-bleeding effects. In *Proceedings of the IEEE/CVF International Conference on Computer Vision (ICCV)*, pages 14667–14676, Montreal, Canada. IEEE.
- [Krizhevsky et al., 2012] Krizhevsky, A., Sutskever, I., and Hinton, G. E. (2012). Imagenet classification with deep convolutional neural networks. In Pereira, F., Burges, C. J. C., Bottou, L., and Weinberger, K. Q., editors, *Advances in Neural Information Processing Systems*, volume 25, Lake Tahoe, Nevada, USA. Curran Associates, Inc.
- [Larsson et al., 2016] Larsson, G., Maire, M., and Shakhnarovich, G. (2016). Learning representations for automatic colorization. In *European Conference on Computer Vision (ECCV)*, Amsterdam. Springer Science+Business Media.
- [Lee et al., 2020] Lee, J., Kim, E., Lee, Y., Kim, D., Chang, J., and Choo, J. (2020). Reference-based sketch image colorization using augmented-self reference and dense semantic correspondence. In *2020 IEEE/CVF Conference on Computer Vision and Pattern Recognition (CVPR)*, pages 5800–5809, Virtual Conference. IEEE.
- [Li et al., 2019] Li, B., Lai, Y.-K., John, M., and Rosin, P. L. (2019). Automatic example-based image colorization using location-aware cross-scale matching. *IEEE Transactions on Image Processing*, 28(9):4606–4619.
- [Mann and Whitney, 1947] Mann, H. B. and Whitney, D. R. (1947). On a Test of Whether one of Two Random Variables is Stochastically Larger than the Other. *The Annals of Mathematical Statistics*, 18(1):50 – 60.
- [Martin et al., 2001] Martin, D., Fowlkes, C., Tal, D., and Malik, J. (2001). A database of human segmented natural images and its application to evaluating segmentation algorithms and measuring ecological statistics. In *Proc. 8th Int’l Conf. Computer Vision*, volume 2, pages 416–423, Vancouver. IEEE.
- [Özbulak, 2019] Özbulak, G. (2019). Image colorization by capsule networks. In *IEEE Conference on Computer Vision and Pattern Recognition Workshops, CVPR Workshops 2019, Long Beach, CA, USA, June 16-20, 2019*, pages 2150–2158, Long Beach, CA, USA. Computer Vision Foundation / IEEE.
- [Pedregosa et al., 2011] Pedregosa, F., Varoquaux, G., Gramfort, A., Michel, V., Thirion, B., Grisel, O., Blondel, M., Prettenhofer, P., Weiss, R., Dubourg, V., et al. (2011). Scikit-learn: Machine learning in python. *Journal of machine learning research*, 12(Oct):2825–2830.
- [Sheikh et al., 2006] Sheikh, H., Sabir, M., and Bovik, A. (2006). A statistical evaluation of recent full reference image quality assessment algorithms. *IEEE Transactions on Image Processing*, 15(11):3440–3451.
- [Simonyan and Zisserman, 2015] Simonyan, K. and Zisserman, A. (2015). Very deep convolutional networks for large-scale image recognition. In *3rd International Conference on Learning Representations, ICLR 2015, San Diego, CA, USA, May 7-9, 2015, Conference Track Proceedings*, San Diego, CA, USA. ICLR.
- [Spearman, 1904] Spearman, C. (1904). The proof and measurement of association between two things. *The American Journal of Psychology*, 15(1):72–101.

- [Su et al., 2020] Su, J.-W., Chu, H.-K., and Huang, J.-B. (2020). Instance-aware image colorization. In *Proceedings of the IEEE/CVF Conference on Computer Vision and Pattern Recognition (CVPR)*, Virtual Conference. Computer Vision Foundation / IEEE.
- [Van der Walt et al., 2014] Van der Walt, S., Schönberger, J. L., Nunez-Iglesias, J., Boulogne, F., Warner, J. D., Yager, N., Gouillart, E., and Yu, T. (2014). scikit-image: image processing in python. *PeerJ*, 2:e453.
- [Vitoria et al., 2020] Vitoria, P., Raad, L., and Ballester, C. (2020). Chromagan: Adversarial picture colorization with semantic class distribution. In *The IEEE Winter Conference on Applications of Computer Vision (WACV)*, Snowmass Village, USA. IEEE.
- [Wang et al., 2004] Wang, Z., Bovik, A. C., Sheikh, H. R., and Simoncelli, E. P. (2004). Image quality assessment: From error visibility to structural similarity. *Trans. Img. Proc.*, 13(4):600–612.
- [Wang et al., 2003] Wang, Z., Simoncelli, E., and Bovik, A. (2003). Multiscale structural similarity for image quality assessment. In *The Thirty-Seventh Asilomar Conference on Signals, Systems Computers, 2003*, volume 2, pages 1398–1402 Vol.2, Pacific Grove, CA, USA. IEEE.
- [Welsh et al., 2002] Welsh, T., Ashikhmin, M., and Mueller, K. (2002). Transferring color to greyscale images. *ACM Trans. Graph.*, 21(3):277–280.
- [Wu et al., 2019] Wu, M., Jin, X., Jiang, Q., Lee, S.-J., Guo, L., Di, Y., Huang, S., and Huang, J. (2019). Remote sensing image colorization based on multiscale senet gan. In *2019 12th International Congress on Image and Signal Processing, BioMedical Engineering and Informatics (CISP-BMEI)*, pages 1–6, Suzhou, China. IEEE.
- [Wu et al., 2021] Wu, Y., Wang, X., Li, Y., Zhang, H., Zhao, X., and Shan, Y. (2021). Towards vivid and diverse image colorization with generative color prior. In *Proceedings of the IEEE/CVF International Conference on Computer Vision (ICCV)*, pages 14377–14386, Montreal. Computer Vision Foundation / IEEE.
- [Yatziv and Sapiro, 2006] Yatziv, L. and Sapiro, G. (2006). Fast image and video colorization using chrominance blending. *IEEE Transactions on Image Processing*, 15(5):1120–1129.
- [Yoo et al., 2019] Yoo, S., Bahng, H., Chung, S., Lee, J., Chang, J., and Choo, J. (2019). Coloring with limited data: Few-shot colorization via memory augmented networks. In *2019 IEEE/CVF Conference on Computer Vision and Pattern Recognition (CVPR)*, pages 11275–11284, Los Alamitos, CA, USA. IEEE Computer Society.
- [Zhang et al., 2016] Zhang, R., Isola, P., and Efros, A. A. (2016). Colorful image colorization. *CoRR*, abs/1603.08511.
- [Zhang et al., 2018] Zhang, R., Isola, P., Efros, A. A., Shechtman, E., and Wang, O. (2018). The unreasonable effectiveness of deep features as a perceptual metric. In *2018 IEEE/CVF Conference on Computer Vision and Pattern Recognition*, pages 586–595, Salt Lake City, UT, USA. Computer Vision Foundation / IEEE.
- [Zhang et al., 2017] Zhang, R., Zhu, J.-Y., Isola, P., Geng, X., Lin, A. S., Yu, T., and Efros, A. A. (2017). Real-time user-guided image colorization with learned deep priors. *ACM Trans. Graph.*, 36(4).
- [Zhao et al., 2020] Zhao, J., Han, J., Shao, L., and Snoek, C. G. M. (2020). Pixelated semantic colorization. *International Journal of Computer Vision*, 128(4):818–834.
- [Zhao et al., 2018] Zhao, J., Liu, L., Snoek, C., Han, J., and Shao, L. (2018). Pixel-level semantics guided image colorization. In *British Machine Vision Conference 2018, BMVC 2018, Newcastle, UK, September 3-6, 2018*, page 156, Newcastle, UK. BMVA Press.